Automatic Differentiation as a Tool for Sensitivity Analysis of a Convective Storm in a 3-D Cloud Model*

Seon Ki Park† Kelvin K. Droegemeier† Christian H. Bischof‡

Argonne Preprint ANL/MCS-P582-0496§

Abstract

The ADIFOR automatic differentiation tool is applied to a 3-D storm-scale meteorological model to generate a sensitivity-enhanced code capable of providing derivatives of all model output variables and related diagnostic (derived) parameters as a function of specified control parameters. The tangent linear approximation, applied to a deep convective storm by the first of its kind using a full-physics compressible model, is valid up to 50 min for a 1 % water vapor perturbations. The result is very encouraging considering the highly nonlinear and discontinuous properties of solutions. The ADIFOR-generated code has provided valuable sensitivity information on storm dynamics. Especially, it is very efficient and useful for investigating how a perturbation inserted at earlier time propagates through the model variables at later times. However, it is computationally very expensive to be applied to the variational data assimilation, especially for 3-D meteorological models, which potentially have a large number of input variables.

Keywords: tangent linear approximation, forward sensitivity, adjoint sensitivity, vartiational data assimilation, convective storm, 3-D cloud model, moist convection, supercell storm

1 Introduction

The dynamical evolution of numerically simulated storms is highly dependent on the physical and computational parameters in the model, as well as on the initial and boundary conditions. The deterministic approach to sensitivity analysis, which employs both the tangent linear and adjoint of the original nonlinear model, can provide a wealth of sensitivity information at a very low cost compared with traditional brute force and Monte Carlo methods, which make numerous simulations with the full numerical model and perform various types of statistical analysis on the output.

---

§To appear in *Computational Differentiation: Techniques, Applications, and Tools*, M. Berz, C. Bischof, G. Corliss, and A. Griewank, Eds., SIAM, Philadelphia, 1996.

*This work was supported by the Center for Analysis and Prediction of Storms at the University of Oklahoma under Grant ATM91-20009 from the National Science Foundation (NSF), by a supplemental grant through the NSF from the Federal Aviation Administartion, and by the Mathematical, Information, and Computational Sciences Division subprogram of the Office of Computational and Technology Research, U.S. Department of Energy, under Contract W-31-109-Eng-38.

†School of Meteorology and Center for Analysis and Prediction of Storms, University of Oklahoma, Norman, OK 73019, {spark,kdroege}@uokmor.edu.

‡Mathematics and Computer Science Division, Argonne National Laboratory, 9700 S. Cass Ave., Argonne, IL 60439, bischof@mcs.anl.gov.

In the deterministic approach, one develops a set of differential sensitivity equations, which is used to express the gradient of the solution vector with respect to input parameters [21]. Sensitivity coefficients are then computed exactly by solving the differential equations using a nonlinear solution as a basic state (e.g., [8, 17, 5]). In this sense, the sensitivity is defined as the gradient (i.e., the first-order derivative) of the model response with respect to any input parameter [18].

The gradients can be computed efficiently and accurately by using automatic differentiation (AD) tools, which apply the chain rule systematically to elementary operations or functions to generate derivative codes of given nonlinear models [2]. Besides providing basic sensitivity information, AD tools are indispensable in variational data assimilation, whose optimization processes require accurate gradient information.

In meteorology, the adjoint model (ADJM) has been used substantially in both sensitivity analysis (e.g., [8]) and variational data assimilation (e.g., [14]). Although AD tools exist for generating the ADJM (e.g., Odyssée [19], AMC [10]), the ADJMs, especially of 3-D models, are still routinely generated by hand. Bischof et al. [5] have successfully applied an AD tool to generate the tangent linear model (TLM) of a 3-D mesoscale model (the PSU/NCAR MM5). A compilation of currently available AD tools can be found in [4] and on the World Wide Web at

`http://www.mcs.anl.gov/Projects/autodiff/AD_Tools`.

In this study, we apply the ADIFOR (Automatic DIfferentiation of FORtran) general-purpose AD tool [2, 3] to the 3-D Advanced Regional Prediction System (ARPS) [22] to generate a sensitivity-enhanced (SE-ARPS) code capable of providing derivatives of all model output variables and related diagnostic (derived) parameters as a function of specified control parameters, including initial and boundary conditions as well as physical and computational constants.

In this manner, we obtain exact derivative information, which is used to establish physical/dynamical cause and effect between changes in input and changes in output. Specifically, we compute the sensitivity of model outputs with respect to water vapor, which is a major factor to control storm life and morphology. We also compute sensitivities of the cost function, which measures distance in the Euclidean norm between the observation data and model results, with respect to all forecast aspects. Subsequently, we discuss implications of the sensitivity results on data assimilation.

ARPS is a fully compressible cloud model with full physics. Although an AD tool has been applied to a nonhydrostatic mesoscale model [5], no AD tool has been applied to a compressible model. In a compressible model, meteorologically unimportant acoustic waves are also supported, which severely limit the timestep size of explicit time integration schemes. To improve efficiency, ARPS employs the mode-splitting time integration technique [13]. In this technique, a large integration timestep is divided into a number of small timesteps; the acoustically active terms are updated every small timestep, while all other terms are computed only once every large timestep. This research is the first of its kind to apply an AD tool to a storm-scale model (meteorologically) with a mode-splitting time integration scheme (computationally).

2 Automatic Differentiation – ADIFOR

Developing the adjoint model by hand is tedious, time-consuming, and error-prone work, especially for a large model such as ARPS, which is composed of more than two hundred subroutines. We therefore use ADIFOR to compute sensitivities of all given dependent

variables (DVs, e.g., forecast aspects and their diagnostic functions) with respect to all given independent variables (IVs, e.g., initial and boundary conditions). For a single run, ADIFOR performs one control run and as many TLM runs as the number of IVs, implicitly. The final results are exactly the same as would be obtained from as many ADJM runs as the number of DVs. In meteorology, ADIFOR has been applied to a 1-D convective cloud model [17, 16], a 3-D storm-scale model [15], a mesoscale model [5], and an air quality model [11].

3 Methodology – Sensitivity to Perturbations

In the context of 3-D models, the number of IVs is potentially very large when grid variables are considered, and this may inhibit the practical computation of sensitivity because of memory limitations. We propose to compute sensitivities with respect to the perturbations inserted in model variables rather than the grid variables themselves. That is, by introducing an artificial perturbation parameter, e, into the original forward model (ARPS), ADIFOR can generate a sensitivity code that regards e as one of the IVs [5].

Consider, for example, the water vapor field, Q_v. If we perturb it by a factor e,

$$Q_v(x, y, z, t; e) = (1 + e)Q_v(x, y, z, t), \tag{1}$$

any quantity P that is influenced by the water vapor field implicitly depends upon e. Expanding $P(e)$ in a Taylor series about the reference state $[P(e = 0)]$ and retaining only the first-order term, we obtain an approximation of the sensitivity of P with respect to e:

$$\delta P(x, y, z, t) = \left.\frac{\partial P(x, y, z, t; e)}{\partial e}\right|_{e=0}. \tag{2}$$

Here, δP can be interpreted as the sensitivity of P to a uniform relative change in the water vapor field. We have modified the ARPS to include e as an input parameter, as shown in (1), and have applied ADIFOR to differentiate this code with respect to e.

Since the perturbation e is added to the input parameters, which already have their own characteristic distribution in the model domain, sensitivities computed from this approach implicitly involve the effect of distribution for those parameters. We limit our experiments only to initial conditions. Boundary conditions, including lateral, top, and bottom, are excluded for sensitivity experiments and TLM validation.

We also compute sensitivities of the cost function with respect to perturbations in all forecast aspects. The cost function, J, is defined as the squared distance between the model state, $\vec{X}$, and the corresponding observations, $\vec{X}^o$:

$$J = \sum_{n=1}^{N} < W_{\vec{X}}(\vec{X}_n - \vec{X}_n^o), (\vec{X}_n - \vec{X}_n^o) >, \tag{3}$$

where $<\vec{A}, \vec{B}>$ denotes a scalar product between $\vec{A}$ and $\vec{B}$ and n represents the time index. Here, the scalar product implies the sum of the products of corresponding components of the two vectors [9]. $W_{\vec{X}}$ is a weighting factor matrix, where $W_{\vec{X}} = (W_u, W_v, W_w, W_\theta, W_p, W_{Q_v}, W_{Q_c}, W_{Q_r})^T$ for the 3-D ARPS with subscripts corresponding to model variables, where u, v, and w are the Cartesian components of velocity, θ is the potential temperature, p is the pressure, Q_v, Q_c and Q_r are mixing ratios of water vapor, cloud water, and rain water, respectively.

The weight for the vertical velocity, W_w, for example, is computed following Wang [20],

$$W_w = \left[8 \sum_{n=1}^{N} \sum_{k=1}^{K} (w_{n,k} - w_{n,k}^{o})^2 \right]^{-1}, \tag{4}$$

with similar expressions for other variables. Here, k denotes the grid space index. In this manner, the cost function is nondimensionalized and becomes unity at the beginning of the variational data assimilation window.

4 3-D Storm Model and Control Run

Our experiments are performed using the sensitivity-enhanced code generated from Version 4.0 of the ARPS, which is three dimensional, fully compressible, and nonhydrostatic. The prognostic variables, solved on the Arakawa C grid [1], include Cartesian velocity components, perturbations of potential temperature and pressure, mixing ratios of water vapor, cloud water, and rain water, and turbulent kinetic energy. The advective modes are computed on large timesteps with a leap-frog time scheme and second-order centered space differencing, whereas the acoustic modes are integrated on small timesteps with an implicit scheme. Kessler-explicit warm-rain microphysics is employed [12]. An extensive description of the model can be found in the ARPS users guide [22].

The computational domain consists of 53×53 grids in the horizontal with a grid size of 1 km. In the vertical, a stretched grid system is employed for 35 grids with a resolution of 150 m near the ground and 850 m at the top of the model domain. The model is run for 140 min, with a large timestep of 6 sec and a small timestep of 1 sec. The detailed model configuration for our experiments is described in [15].

The simulation to verify the computation of derivatives by ADIFOR is made by using the HALF4 (supercell) hodograph and thermodynamic sounding from [7], the latter of which has a surface mixing ratio of 15 g/kg. This wind profile consists of a semi-circular arc of 10 m/s radius that turns clockwise over the lowest 4 km starting with the surface easterly winds. The (westerly) wind is constant, with height above 4 km at a speed of 10 m/s. The convection is initiated by a 4 K thermal perturbation placed in the boundary layer. The simulated supercell develops rapidly during the first 30 minutes and becomes quasi-steady thereafter, with a sustained updraft of around 47 m/s. In Figure 1, the surface outflow boundary velocity and vertical velocity at 4 km are depicted for $t = 50$ and 120 min. The storm moves to the west initially and then turns northeastward as it grows in vertical extent, forming a strong surface cold pool.

Another storm is triggered by convergence along the northern gust front. Also, as the northeast part of the gust front intensifies, a new cell develops along it ($t = 50$ min; Figure 1a), constituting three distinct cells. As the northern part of the gust front moves northward out of the model domain by 60 min, the two northern storms decay, and other weak secondary storms mill around the northern lateral boundary. The dominant storm thereafter is the isolated supercell, which travels southeastward along the leading edge of the expanding cold pool. A secondary storm develops northeast of the main storm after 100 min (Figure 1b), merging into the main storm by 140 min.

5 TLM Validation

Before we proceed to the sensitivity computation, we validate the TLM solutions computed by the ADIFOR-generated code, which describe the linear evolution of perturbations. The

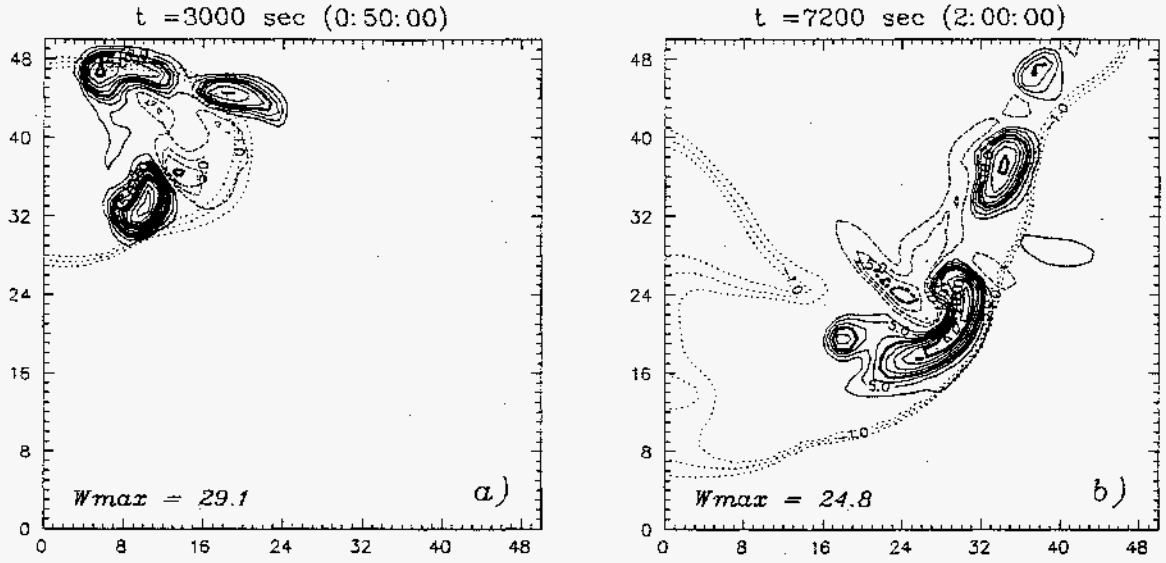

FIG. 1. *Control simulation: vertical velocity at 4 km (positive in solid and negative in dashed lines at an interval of 2.5 m/s) and perturbation potential temperature (dotted lines with contours larger than -2.0 K at an interval of 0.5 K) at (a) 50 min and (b) 120 min*

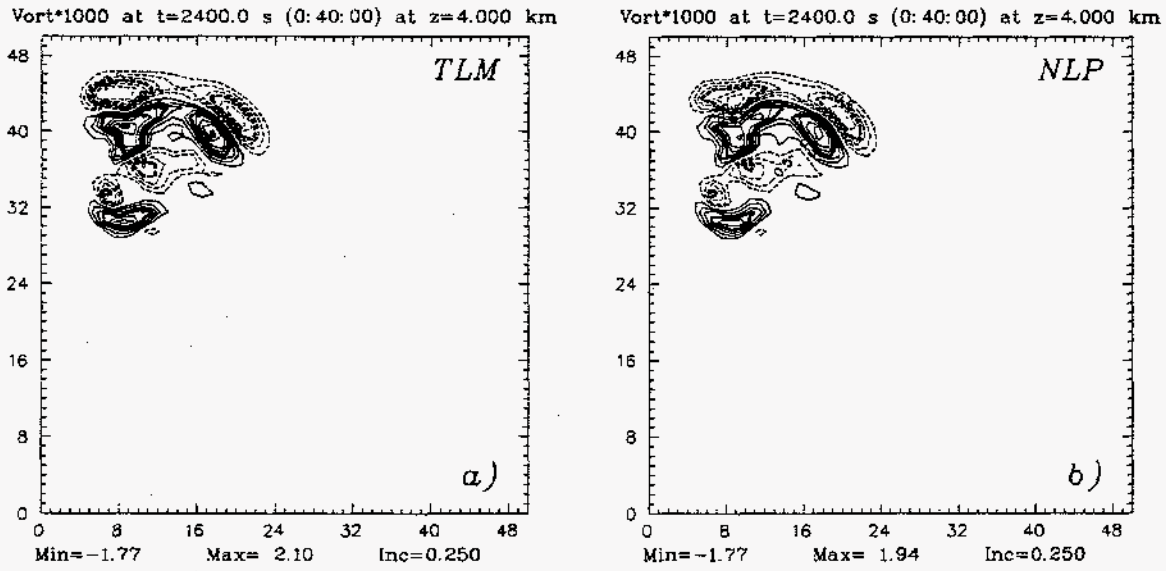

FIG. 2. *x-y slices (at $z = 4.0$ km) of (a) tangent linear perturbation and (b) nonlinear perturbation in vorticity at $t = 40$ min for a 1 % perturbation in initial water vapor (in s^{-1})*

validation is carried out by comparison with the nonlinear perturbation (NLP) fields; the difference fields computed between the nonlinear control run and another nonlinear run whose initial state is slightly perturbed from it.

Figure 2 shows the TLM and NLP fields of vorticity at 40 min for a 1% perturbation (bias-type) in water vapor over the whole model domain except for the lateral, top, and bottom boundaries. They are plotted on an x-y plane at $z = 4.0$ km.

The two fields agree quite well in both magnitude and location. However, after about 55 min, the solutions begin to diverge. That is, in reality, the perturbations and (time-

evolving) nonlinear base state interact to a significant extent, and the absence of this interaction in the TLM leads to erroneous results. The correlation drops rapidly below 0.9 after about 45 min. In a case without subgrid-scale turbulent mixing, which is a highly nonlinear process, the time over which the two fields agree increases.

6 Sensitivity Results

We now investigate the effect of perturbations introduced in the water vapor field in different regions of storm environments on storm dynamics. The water vapor field is a major factor for storm life and morphology. We introduce four perturbation equations following the equation (1) for four different regions in the model: (e_1) inside the rain region ($Q_r > 1e^{-4}$ g g^{-1}) above the cloud base, (e_2) in the ambient environment outside the rain region and above the cloud base, (e_3) the updraft region (including $w = 0$) in the subcloud layer, and (e_4) the downdraft region in the subcloud layer. For the cost function, sensitivities are computed for perturbations in all forecast aspects (i.e., $e_u, e_v, e_w, e_\theta, e_p, e_{Q_v}, e_{Q_c}$, and e_{Q_r}) both inside and outside the rain region of the storm.

To investigate the sensitivity of our storms to perturbations in the water vapor, we run the SE-ARPS starting at 50 min, i.e., the effect of the perturbation begins when the storm is in its developing stage (see Figure 1a). Among the many available results, we investigate the sensitivity of ground rainfall (GR) to water vapor perturbations in the four regions described above.

The cloud base at 50 min is around 640 m. Four model levels are involved in the subcloud layer (excluding the bottom boundary). The numbers of grid points involved in perturbation are 8280 for e_1, 61720 for e_2, 5972 for e_3, and 4028 for e_4.

The amount and location of ground rainfall are among the most important quantities in storm-scale prediction. Figure 3 shows the sensitivity of GR at 120 min with respect to the previous four perturbations inserted at 50 min. Recall that, at 120 min, the main updraft is located near the center of the domain with a lima-bean shape, while a secondary storm develops to the west (see Figure 1b). Also, a prominent secondary storm exists to the northeast of the main storm, along with another weak storm near the northern lateral boundary.

Among all perturbations, the largest sensitivity of GR is due to the e_1 perturbation. For vapor perturbations inside the rain region (e_1), the major increase in GR occurs in the secondary storm with a maximum of 527 mm (Figure 3a). The GR decreases at the weak downdraft region to the north of the main storm with a minimum of -479 mm. This indicates that a 1% moisture perturbation inside the rain region above the cloud base at $t = 50$ min induces a maximum increase of 5.27 mm and a decrease of 4.79 mm in the secondary storm rainfall at $t = 120$ min.

The major influence of the e_2 perturbation occurs in the main storm area, with a large increase beneath the main storm and a decrease in the western part and north of the storm (Figure 3b). Both the e_3 and e_4 perturbations result in a decrease below the main storm and increase below the secondary storm in the west (Figures 3c and 3d). The sensitivity to the e_3 perturbation is about three times larger than that to the e_4 perturbation. The e_4 perturbation also increases GR at the region of north secondary storm.

Overall, the largest influence on GR comes from the e_1 perturbation, but at the secondary storm to the north. For the main storm, while the moisture perturbation in the ambient environment above the cloud base (e_2) increases the ground rainfall, the perturbations in both the updraft and downdraft region below the cloud base (e_3 and e_4)

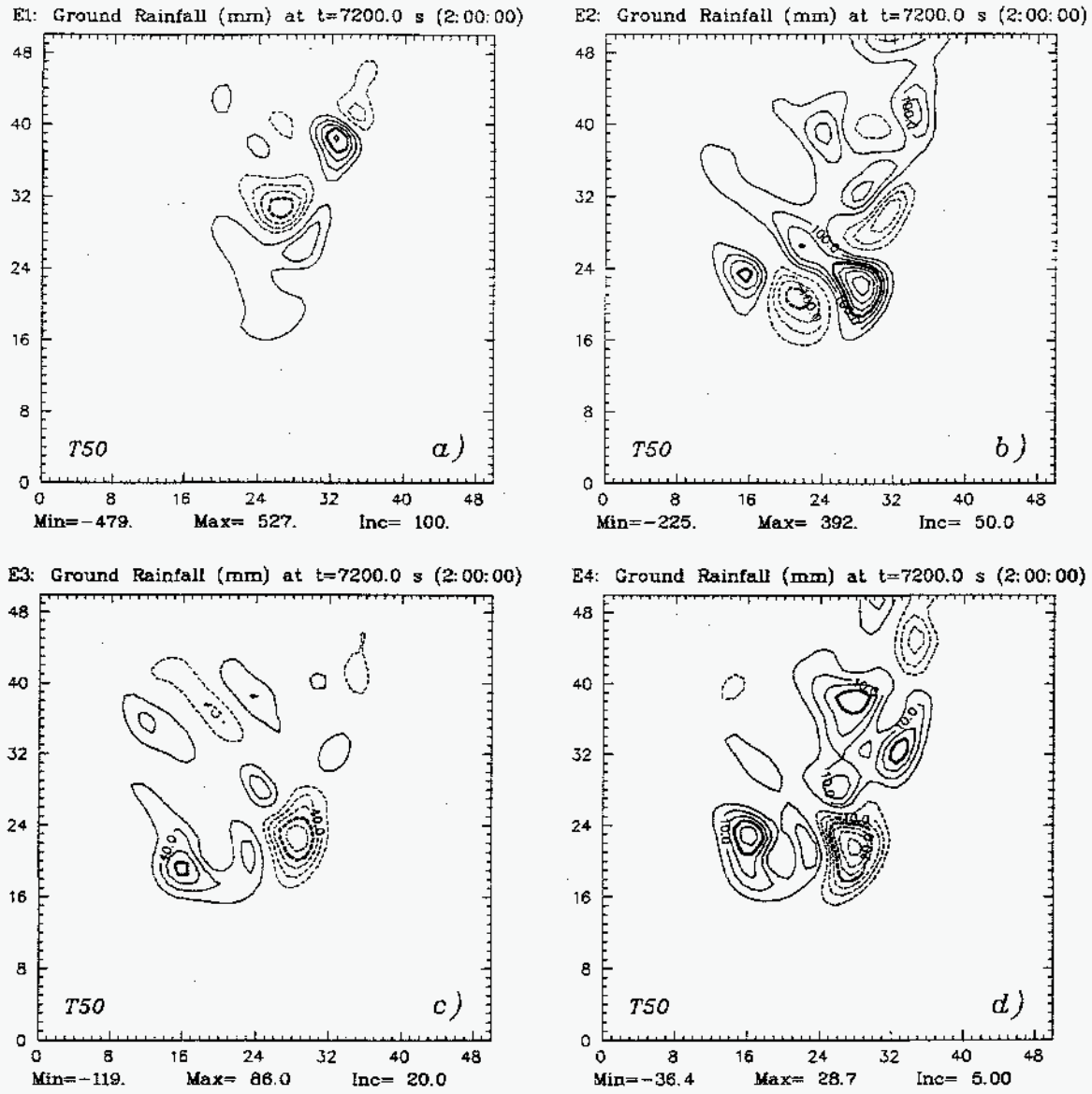

FIG. 3. *Sensitivities of ground rainfall at* $t = 120$ *min with respect to the moisture perturbations of (a)* e_1*, (b)* e_2*, (c)* e_3 *and (d)* e_4 *at* $t = 50$ *min (in mm)*

decrease the ground rainfall at 120 min.

We now discuss the sensitivity results in the cost function and their implications on data assimilation. We consider the control simulation (see Figure 1) as our pseudo-observations. The sensitivity period is 30 min, from $t = 80$ min to $t = 110$ min. A 1% perturbation is added to all variables at all grid points at 80 min for the perturbation run, which serves as the nonlinear basic field for the sensitivity computation.

With this perturbation, model solutions show little difference from the observations. Note that ARPS actually predicts the perturbations of potential temperature (θ) and pressure (p). Since the total fields of θ and p are observed in practice (i.e., base state + perturbation), we specify their total fields as independent variables for the sensitivity computation rather than using the perturbation fields.

TABLE 1

Sensitivity of cost function at 110 min with respect to the perturbations of forecast aspects at 80 min both inside (IN) and outside (OUT) the rain region

	$\partial J/\partial e_u$	$\partial J/\partial e_v$	$\partial J/\partial e_w$	$\partial J/\partial e_\theta$	$\partial J/\partial e_p$	$\partial J/\partial e_{Q_v}$	$\partial J/\partial e_{Q_c}$	$\partial J/\partial e_{Q_r}$
IN	.0069	-.281	.043	143.4	25.47	3.78	-.013	-.32
OUT	-.68	.188	-.003	-107.7	-.74	-4.63	.0008	-.0011

The weight functions computed from (4) for this experiment are $W_u = 7.21 \times 10^{-8}$ $(\mathrm{m/s})^{-2}$, $W_v = 5.12 \times 10^{-8}$ $(\mathrm{m/s})^{-2}$, $W_w = 9.66 \times 10^{-8}$ $(\mathrm{m/s})^{-2}$, $W_\theta = 3.02 \times 10^{-7}$ K^{-2}, $W_p = 2.66 \times 10^{-11}$ Pa^{-2}, $W_{Q_v} = 1.90$ $(\mathrm{g/g})^{-2}$, $W_{Q_c} = 14.36$ $(\mathrm{g/g})^{-2}$, and $W_{Q_r} = 0.87$ $(\mathrm{g/g})^{-2}$. As defined in (4), the weight function of any variable is inversely proportional to the amount of forecast error in that variable, which is summed from the perturbation insertion time to the verification time.

In Table 1, we show the adjoint sensitivities of the cost function (J) at 110 min to perturbations at 80 min in specified variables both inside (IN) and outside (OUT) the rain region. Because they are nondimensional and the cost function is unity at this time (110 min), we can compare the relative importance among variables.

For the perturbations inside the rain region, the largest sensitivity in the cost function (i.e., forecasting error) is due to errors in potential temperature (θ), followed by pressure (p) and water vapor (Q_v). The sensitivities are positive for all three perturbations. Among all variables, the cloud water (Q_c) perturbation exerts the smallest effect on the cost function. Among the moisture variables inside the cloud, water vapor exerts the largest influence on J, followed by rainwater (Q_r) and cloud water.

Perturbations in the momentum variables (u, v and w) inside the rain region yield small changes in J. Among them, the largest sensitivity of J is due to the v perturbation, and the smallest is due to the u perturbation. For perturbations outside the rain region, the sensitivities are generally smaller than those for perturbations inside the rain region, except for the sensitivity to the u perturbation. Note the prominent decrease in the influence on J of perturbations in p. Since Q_c and Q_r are effectively zero in the environment, the sensitivities of J to them are extremely small. The largest sensitivity in the cost function is due to θ, followed by Q_v and p.

The perturbations in θ, Q_v and v outside the rain region induce similar changes in J, but in different directions compared with those inside the rain region. Other variables demonstrate significant changes in sensitivity values. For example, the absolute sensitivity of the cost function to the u perturbation outside the rain region is about 100 times larger than inside the rain region, while the sensitivity to the Q_v perturbation is about 1.2 times larger.

In both cases, the p field has the largest effect on the cost function during the early sensitivity period (not shown). This is because p is directly responsible for the mass balance through the pressure gradient forces in the momentum equations. When p is perturbed, the flow accelerates until terms involving the velocity become comparable with the pressure gradient force. Therefore, the flow immediately and significantly responds to the p perturbations. In contrast, perturbations in θ affect the system initially through only buoyancy term in the vertical momentum equation. That is, p affects all three components of velocity simultaneously through the pressure gradient force, while θ affects only the vertical velocity initially and then other variables through mass continuity. Hence, during the early sensitivity period, the p perturbations exert the largest influence on forecast

errors among all variables. However, the increased buoyancy through the θ perturbation eventually influences storm dynamics and forecast error.

7 Discussion

For the deep convective storm studied here, the tangent linear solutions, which describe the evolution of perturbations along trajectories of a time-dependent nonlinear base state, represent the corresponding nonlinear perturbation fields very accurately up to about 50 min for a 1% moisture perturbation. Considering the highly nonlinear and discontinuous properties of solutions in a full-physics nonhydrostatic cloud model such as ARPS, these results are encouraging for future studies of storm predictability, data assimilation, Doppler radar retrieval, and ensemble forecasting, all of which require derivative or sensitivity information.

In the supercell simulation, bias-type errors in the water vapor in different regions of the model exert influences on storm dynamics in different ways. Perturbations introduced inside the rain region above cloud base mostly affect the secondary cells, while those outside the rain region mainly influence the main storm. When the perturbations are introduced in the subcloud layer, both the main and secondary cells are affected. Among the vapor perturbations in different regions, the perturbations inside the rain region have the largest influence on storm dynamics.

These results imply that we may need high-quality vapor data from either observations or retrievals in order to obtain accurate predictions of storm behavior. The required accuracy of water vapor can be estimated once the criteria on the forecast accuracy is determined. For example, suppose that a relative sensitivity of the forecast error [15] to water vapor is 20, which implies that the forecast error changes by 20% as a result of a 1% error in water vapor. If one wishes a forecast with only a 10% error, the observation for water vapor should have an error smaller than 0.5%.

For perturbations inside the rain region, the cost function showed the largest sensitivity with respect to temperature, followed by pressure and then water vapor. For perturbations in ambient environment, the cost function showed the largest sensitivity to temperature, followed by water vapor and then pressure. All other variables have almost negligible effect on the cost function. This result is also demonstrated in our 1-D experiments [16].

When applied to variational data assimilation, sensitivity information, especially derivatives of the cost function with respect to all initial fields, can indicate which initial field must be modified by a large amount and which may be altered by only a small amount to change a specific amount of cost function on the way to its minimum state. With this information, the minimization algorithm can be appled in a selective way to save computing times: that is, a variable that exerts little influence on the cost function may be put in the minimization process in a larger iteration step, while a variable with strong effect (especially temperature) may be applied in every step.

Even though ADIFOR does not produce the adjoint, it gives more information than handcoded tangent linear or adjoint models. In our experience, an AD tool dispenses with much labor and time in handcoding the adjoint model, yet provides a great amount of gradient information needed for sensitivity analysis and data assimilation. Compared with the divided-difference approach, AD avoids the difficulty of choosing an optimal perturbation size, to which the solutions of cloud model are extremely sensitive, and also saves a great amount of computing time by avoiding numerous runs with full numerical model. The ADIFOR-generated code is especially efficient and useful for investigating

how a perturbation inserted at any given intermediate time propagates through the model variables at later times. Furthermore, it is demonstrated that automatic differentiation can be applied with no problem to a compressible model using a mode-splitting time integration technique.

In the context of data assimilation especially for 3-D models, however, we note that it is computationally impractical to compute sensitivities with respect to all model grid variables through the ADIFOR-generated code, mainly because of memory limitations. For example, the nonlinear ARPS with $53 \times 53 \times 35$ grids requires about 9.5 MWords on a Cray-C90, while that machine in the Pittsburgh Supercomputing Center has a maximum memory of 512 MWords. Therefore, the maximum number of IVs that can be computed through the SE-ARPS is only about 50. In data assimilation and Doppler radar retrieval, we usually require the gradient information of the cost function with respect to all model grid variables, which constitutes 98315 IVs for only one forecast aspect in our case.

Furthermore, for the purpose of data assimilation, the ADIFOR-generated code is computationally very expensive compared with the pure adjoint model. The reason is that the former is basically a forward model and thus repeats the sensitivity computation implicitly for the number of IVs. Although we may save computing time by applying the sparse matrix option in generating the derivative codes and by using the pseudo-adjoint technique [6], a comparative study has not been performed yet for a 3-D model.

References

[1] A. Arakawa and V. R. Lamb, *Computational design of the basic dynamical processes of the UCLA general circulation model*, in Methods in Computational Physics, 17, Academic Press, 1977, pp. 174–265.

[2] C. Bischof, A. Carle, G. Corliss, A. Griewank, and P. Hovland, *ADIFOR: Generating derivative codes from Fortran programs*, Scientific Programming, 1 (1992), pp. 11–29.

[3] C. Bischof, A. Carle, P. Khademi, and A. Mauer, *The ADIFOR 2.0 system for the automatic differentiation of Fortran 77 programs*, 1994. Preprint MCS-P481-1194, Mathematics and Computer Science Division, Argonne National Laboratory, and CRPC-TR94491, Center for Research on Parallel Computation, Rice University. To appear in IEEE Computational Science & Engineering.

[4] C. Bischof and F. Dilley, *A compilation of automatic differentiation tools*, ACM SIGNUM Newsletter, 30 (1995), pp. 2–20.

[5] C. Bischof, G. Pusch, and R. Knoesel, *Sensitivity analysis of the MM5 weather model using automatic differentiation*, Preprint MCS-P532-0895, Mathematics and Computer Science Division, Argonne National Laboratory, 1995.

[6] C. H. Bischof, *Automatic differentiation, tangent linear models and pseudo-adjoints*, in High-Performance Computing in the Geosciences, F.-X. Le Dimet, ed., vol. 462 of Series C: Mathematical and Physical Sciences, Boston, Mass., 1995, Kluwer Academic Publishers, pp. 59–80.

[7] K. K. Droegemeier, S. M. Lazarus, and R. Davies-Jones, *The influence of helicity on numerically simulated convective storms*, Monthly Weather Review, 121 (1993), pp. 2005–2029.

[8] R. M. Errico and T. Vukicevic, *Sensitivity analysis using an adjoint of the PSU-NCAR mesoscale model*, Monthly Weather Review, 120 (1992), pp. 1644–1660.

[9] B. Friedman, *Principles and Techniques of Applied Mathematics*, John Wiley & Sons, 1956.

[10] R. Giering, *Adjoint model compiler, manual version 0.2, AMC version 2.04*, tech. rep., Max-Planck Institut für Meteorologie, August 1992.

[11] D. Hwang and D. Byun, *Application of automatic differentiation for studying the sensitivity of numerical advection schemes in air quality models*, in Proc. High Performance Computing 1995, Phoenix, AZ, April 9-13, 1995, pp. 52–57.

[12] E. Kessler, *On the distribution and continuity of water substance in atmospheric circulation*,

in Meteorological Monograph, 10, American Meteorological Society, 1969.

[13] J. B. Klemp and R. B. Wilhelmson, *The simulation of three-dimensional convective storm dynamics*, Journal of Atmospheric Sciences, 35 (1978), pp. 1070–1096.

[14] J. M. Lewis and J. C. Derber, *The use of adjoint equations to solve a variational adjustment problem with advective constraints*, Tellus, 37A (1985), pp. 309–322.

[15] S. K. Park, *Sensitivity Analysis of Deep Convective Storms*, PhD thesis, School of Meteorology, University of Oklahoma, 1996.

[16] S. K. Park and K. Droegemeier, *On the use of automatic differentiation to assess parametric sensitivity in convective-scale variational data assimilation*, in Preprints, Proc. 2nd Int. Symp. on Assimilation of Observations in Meteorology and Oceanography, Tokyo, Japan, March 1995., World Meteorological Organization, 1995, p. 111-116.

[17] S. K. Park, K. Droegemeier, C. Bischof, and T. Knauff, *Sensitivity analysis of numerically-simulated convective storms using direct and adjoint methods*, in Preprints, 10th Conference on Numerical Weather Prediction, Portland, Oregon, American Meterological Society, 1994, pp. 457–459.

[18] Y. Ronen, *Uncertainty analysis based on sensitivity analysis*, in Uncertainty Analysis, CRC Press, 1988, pp. 41–70.

[19] N. Rostaing, S. Dalmas, and A. Galligo, *Automatic differentiation in Odyssee*, Tellus, 45a (1993), pp. 558–568.

[20] Z. Wang, *Variational data assimilation with 2-d shallow water equations and 3-d FSU global spectral models*, Tech. Rep. FSU-SCRI-93T-149, Florida State University, Department of Mathematics, December 1993.

[21] B. A. Worley, E. M. Oblow, R. E. Pin, J. E. Maerker, J. E. Horwedel, R. Q. Wright, and J. L. Lucius, *Deterministic methods for sensitivity and uncertainty analysis in large-scale computer models*, in Proc. Conf. on Geostatistical, Sensitivity, and Uncertainty Methods for Ground-Water Flow and Radionuclide Transport Modelling, B. E. Buxton, ed., Battelle Press, 1987, pp. 135–154.

[22] M. Xue, K. K. Droegemeier, V. Wong, A. Shapiro, and K. Brewster, *ARPS 4.0 User's Guide*, Center for Analysis and Prediction of Storms, University of Oklahoma, 1995.